Bulletin of Atmospheric Science and Technology (2020) 1:283–295
https://doi.org/10.1007/s42865-020-00018-1

CASE STUDIES

The 1994 Piedmont flood: an archetype of extreme precipitation events in Northern Italy

F. Grazzini[1,3] · G. Fragkoulidis[2] · V. Pavan[3] · G. Antolini[3]

Received: 18 April 2020 / Accepted: 26 August 2020/ Published online: 1 September 2020

Abstract
Extreme precipitation events (EPEs) are meteorological phenomena of major concern for the densely populated regions of northern and central Italy. Although statistically rare, they tend to be recurrent in autumn and share common characteristics in the large-scale dynamical evolution responsible for their generation. Past studies on EPEs have reported, as the main triggering factor, a meridionally elongated upper-level trough embedded in an incoming Rossby wave packet. In this respect, we show how the meteorological conditions leading to the devastating 1994 Piedmont flood represent a typical flow evolution for this type of extreme events. Exploiting the systematic classification of EPEs recently published by the authors and taking advantage of a new observational dataset, this article revisits the role of the large-scale flow on this and similar cases of past EPEs.

Keywords Extreme precipitation · Floods · Po river · Atmospheric rivers · Rossby wave packets · Downstream development

1 Introduction

The extreme precipitation that affected the Piedmont region, in Northern Italy, in November 1994 led to a destructive flood with significant socioeconomic impacts. Seventy people died, and more than two thousand had to be evacuated. Damage to public and private property was extensive, 150 bridges collapsed or were severely damaged, and more than 5000 head of livestock were lost (Buzzi et al. 1998).

The heaviest precipitation occurred between 4 and 6 of November when several rain gauges in mountainous regions recorded accumulated values above 300 mm/36 h (Buzzi and

✉ F. Grazzini
Federico.Grazzini@lmu.de

[1] Meteorologisches Institut, Ludwig-Maximilians-Universität, Munich, Germany

[2] Institute for Atmospheric Physics, Johannes Gutenberg University Mainz, Mainz, Germany

[3] ARPAE-SIMC, Bologna, Regione Emilia-Romagna, Italy

Tartaglione, 1995). Forty percent of the Piedmont territory received more than 200 mm of rain during the event (Arpa Piemonte 1998). The large-scale circulation was characterized by a Rossby wave with meridional extension from the British Isles to the Iberian Peninsula featuring an elongated trough over Western Europe and a blocking anticyclone over Central Europe. Extreme precipitation events (EPEs), like this one, are typically associated with a strongly confluent flow ahead of a polar cold front concentrating water vapour into a narrow plume, which then interacts with the orography (Krichak et al. 2015). Such a flow can be triggered by a breaking Rossby wave over Western Europe that takes the form of a PV streamer, an elongated filament of high potential vorticity (PV) air (Grazzini, 2007, Martius et al. 2008). Since most of the intense orographic precipitation falls in the prefrontal sector, it is essential to study the characteristics of the flow and the associated water vapour transport.

Based on the EPE categorization presented in Grazzini et al., 2020a; (hereafter, G2020), in which the authors classify EPEs into three categories, in the present paper, we discuss the large-scale circulation characteristics leading to the 1994 Piedmont flood and evaluate its similarities with other cases. Following a statistical approach, Grazzini et al. (2020b) investigated the upstream large-scale precursors which influence the frequency and intensity of EPEs. Revisiting the dynamics of the 1994 event might be useful to reveal the processes leading to such an extreme. Highlighting them is essential in the quest for better predictability and impact assessment of future events.

In this article, we will retrace the evolution of the event starting from the description of the regional precipitation pattern and the corresponding synoptic situation and then investigating the spatiotemporal evolution of the associated wave packet at larger scales. The paper is organized as follows. In Section 2, we describe the dataset and the key variables used to analyse the event. In Section 3, we comment on the observed daily precipitation and classification of the event. In Section 4, we discuss the genesis and characteristics of the synoptic pattern associated with the event, while in Section 5, we highlight the key role of the moisture transport and we contrast this case with more recent analogues. Conclusions follow in Section 6.

2 Data and methods

The atmospheric fields used in this study are retrieved from the ERA5 reanalysis (Hersbach et al. 2020), while precipitation data, upon which the EPE definition is based, are retrieved from the new observational dataset ARCIS (Archivio Climatologico per l'Italia Centro Settentrionale). ARCIS is a recently assembled gridded precipitation dataset (with a resolution of 5 km) derived from 1762 rain gauges from 11 regional networks in Northern-Central Italy and several stations of adjacent Alpine regions (Pavan et al. 2019). The dataset has a daily temporal resolution and covers the period 1961–2015. The input data are checked for quality, time consistency, synchronicity, and statistical homogeneity and then spatially interpolated using a modified Shepard's scheme. The 24-h accumulation period corresponds to the best practice of the Italian Hydrological Service, i.e. from 08 to 08 UTC of the following day.

Based on this dataset, EPEs are defined and classified as follows. Precipitation is aggregated over the official warning areas (WAs) provided by the Italian Department of Civil Protection. This choice, preferable to regular boxes, allows averaging precipitation on subregional hydrological basins which are considered climatologically homogenous. Northern-Central Italy is subdivided into 94 WAs, shown in Fig. 1. EPEs are defined as days with

daily precipitation greater than or equal to the 99th percentile across one or more WAs. Subsequently, the meteorological variables listed in Table 1 are used as predictors for the EPE classification as described in G2020. Among these variables, central in the following considerations is the magnitude of the integrated water vapour transport (IVT), as well as its zonal (IVTe) and meridional (IVTn) components. Their instantaneous fields in ERA5 are computed as the integral (over model levels, from the surface to the top of the atmosphere) of the wind component multiplied by the specific humidity at each level. Positive values of IVTe indicate an eastward flux, and positive IVTn values indicate a northward flux.

3 Observed precipitation and event classification

Figure 1 shows the daily accumulated precipitation patterns that led to the Piedmont flood as analysed with the ARCIS dataset which, compared with the raw data of the dense regional networks, has the advantages of being gridded, spatially homogeneous, and not limited to single administrative regions. The precipitation event is prolonged, with very high intensity, especially during the 24-h period from 5 November 08 UTC to 6 November 08 UTC. In this period, daily values above 300 mm were recorded on the northern and western borders of the Piedmont region associated with persistent orographic uplift, while on the southern side of the region, on the border with Liguria, hourly rates in excess of 30 mm/h were reported in a few stations, due to strong convective activity (Arpa Piemonte, 1998).

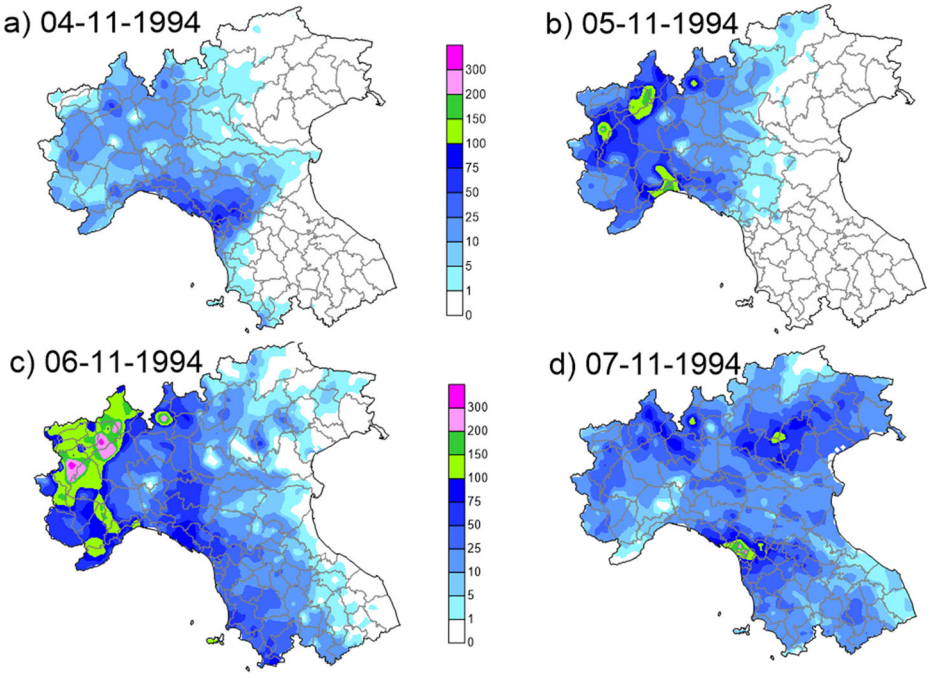

Fig. 1 Gridded daily total precipitation from the ARCIS dataset of high-resolution regional observational networks (mm/24 h). Note that the dates on the panels refer to the end of the 24 h accumulation period 08-08 UTC. The areas in the foregrounds are the Italian Civil Protection Warning Areas used for operational warnings

Table 1 Predictors used in the EPE classification algorithm of G2020

Variable	Description	Units
Tau_{dmax}	Daily maximum convective adjustment time scale	h
$CAPE_{dmax}$	Daily maximum convective available potential energy	J kg^{-1}
IVTe	Daily mean zonal component of integrated water vapour transport (from the surface up to the top of atmosphere)	kg m^{-1} s^{-1}
IVTn	Daly mean meridional component of integrated water vapour transport (from the surface up to the top of the atmosphere)	kg m^{-1} s^{-1}
θ_{e850}	Daily mean equivalent potential temperature at 850 hPa	K
$\Delta\theta_{e500\text{-}850\_dmin}$	Daily minimum θ_e difference between 500 and 850 hPa	K
TCWV	Daily mean total column water vapour	kg m^{-2}
$BS_{500\_925\_dmax}$	Daily maximum wind bulk shear between 500 and 925 hPa	m s^{-1}

For each EPE day, the instantaneous values of the variables are spatially averaged over Northern-Central Italy and aggregated daily, as reported in the table. See G2020 for further details on variable definitions and averaging methods

Compared with the 887 EPEs found in G2020, we notice that the 1994 Piedmont event, although not characterized by an extreme spatial extension (ranked only 32nd in this respect), presents one of the highest area average precipitation intensities. In Table 2 we show precipitation data and the values of atmospheric variables used for the classification of this event. A very similar event, which caused the historical Po river flood in October 2000, is also included in Table 2. The intensity on 5 November 1994 (see the column $mmkm^2$ in Table 2) is just slightly lower and comparable with the one on 14/10/2000, which is the maximum precipitation average intensity recorded among all EPEs.

The next question to address is in which category this event is classified. Here we briefly recall the definition of the three categories in which subdivide EPEs following G2020. Category 1 (Cat1) events originate from intense frontal structures, including slantwise ascent in the warm sector of the associated cyclones (warm conveyor belt). Mechanical (orographic) uplift of low-level marine, statically stable air is the key factor to attain extreme precipitation that is mostly confined over upwind steep topography. Category 2 (Cat2) events originate from

Table 2 Relevant data for two recent historical Po river floods, 4–6 November 1994 and 11–16 October 2000

Day	#WA	Area	$mmkm^2$	IVTe	IVTn	Tau_{dmax}	$CAPE_{dmax}$	TCWV	θ_{e850}	Dtmin	Cat
04/11/1994	7	15.8	68.0	−23.4	148.1	2.2	66.2	23.2	315.5	2.3	2
05/11/1994	*20*	*33.3*	*97.7*	*−66.7*	*234.5*	*4.7*	*97.2*	*21.6*	*314.2*	*3.7*	*2*
06/11/1994	9	12.7	66.6	−24.6	150.5	1.3	77.6	19.8	309.8	5.1	2
11/10/2000	8	11.3	77.1	198.4	208.7	1.3	63.2	19.5	311.3	8.8	2
12/10/2000	3	3.0	61.0	148.9	281.1	4.5	220.0	21.5	317.4	1.0	2
13/10/2000	7	9.3	94.8	−20.0	306.3	6.7	319.5	23.0	320.3	−1.9	2
14/10/2000	*17*	*32.4*	*103.4*	*−120.8*	*296.1*	*5.1*	*184.9*	*25.7*	*321.2*	*0.5*	*2*
15/10/2000	12	23.9	69.9	−153.8	254.2	2.5	114.6	23.3	316.8	3.2	2

#WA number of warning areas with spatial daily average precipitation exceeding the 99th percentile of the respective climatological distribution, *Area* total area exceeding the 99th percentile of daily precipitation [10^3 km^2], *mmkm²* mean area daily precipitation intensity [mm/24 h km^2], *IVTe* mean zonal component of IVT [kg s^{-1} m^{-1}], *IVTn* mean meridional component of IVT [kg s^{-1} m^{-1}], Tau_{dmax}, maximum daily value of Tau [hours], $CAPE_{dmax}$ daily maximum value of CAPE [J/kg], *TCWV* daily mean of total column water vapour [kg/m^2], θ_{e850} daily mean of equivalent potential temperature at 850 hPa [K], *Dtmin* daily minimum of $\Delta\theta_e$ [K] ($\Delta\theta_e = \theta_{e500} - \theta_{e850}$), *Cat* the EPE category. Atmospheric variables are spatially averaged over Northern-Central Italy (roughly corresponding to the area covered by ARCIS dataset) and aggregated daily. The maximum intensity days of the two events are in italics

a synergic combination of frontal uplift and embedded deep convection. They are characterized by a stronger southerly flow component and a reduced moist static stability (almost neutral conditions). Category 3 (Cat3) events are associated with weakly forced convection (non-equilibrium convective events) in a potentially unstable environment (i.e. with very high CAPE). According to the classification method, which is based on the dynamic and thermodynamic predictors listed in Table 1, all the days of the 1994 Piedmont flood episode, as well as the days of the October 2000 event, qualify as Cat2 EPE days, as indicated in Table 2.

In order to provide further evidence for the classification of the event and describe in more detail the relevant processes, Fig. 2 displays the patterns of the ERA5 reanalysis low-level wind at 18 UTC on 5 November 1994 (panel b) and the 06–24 UTC accumulated precipitation from the ERA5 forecast initiated at 06 UTC of the same day (panel a). The precipitation pattern shows two main precipitation areas, on the northern side of the Piedmont region, indicated by the grey arrow, and on the southern side, on the border with Liguria, indicated by the yellow arrow (also evident in Fig. 1b). The partition of precipitation to convective and large scale (or "stratiform") is based on the corresponding definitions and numerical schemes used in ECMWF forecasts and ERA5 (Owens and Hewson, 2018). The red-dashed contours, which indicate the convective fraction, suggest that these two peaks are attributable to two distinct processes. The precipitation peak indicated by the grey arrow is mainly due to orographically enhanced stratiform precipitation which may have had some isolated convective element in it, while the other peak indicated by the yellow arrow lies just on the border of a region where deep convection is predominant (up to 80% of the precipitation amount resulted from the convection scheme of the model).

Figure 2 b provides further information on the observed differences in precipitation type. The red isoline, representing the values of 2 potential vorticity units (PVU) at 330 K, marks the position of the forward side of the upper-level trough (see also Fig. 3). Ahead of it, the cold

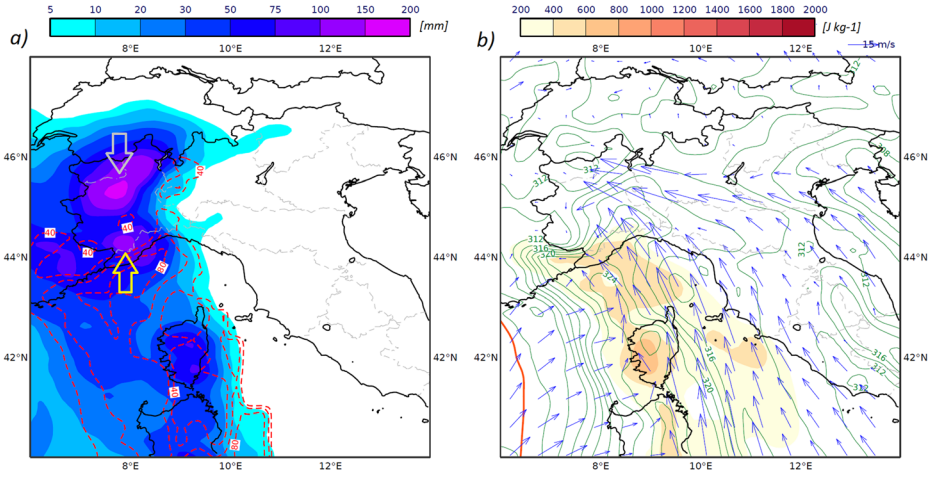

Fig. 2 **a** 18-h accumulated precipitation from 06 UTC to 24 UTC 5 November 1994 in the ERA5 short-term forecast initialized at 06 UTC. The shaded field depicts the total precipitation (mm), while the red dashed contours indicate the convective fraction estimated as the ratio of the convective over the total precipitation in ERA5. Isolines are drawn every 20%, starting from 40%. **b** Synoptic situation derived from the ERA5 hourly reanalysis and valid at 18 UTC of the same day, at about the time of maximum convergence of the southerly and easterly branch of the low level jets. The shaded field is CAPE [J kg^{-1}], the arrows indicate the wind vectors at 925 hPa, the green contours are θ_e at 850 hPa (every 2 K), and the red contours mark the 2PVU contour at 330 K

front is evident and represented by the tight zonal gradient in θ_e at 850 hPa, indicated by the green contours. A key feature is the very intense low-level flow (blue arrows) at 925 hPa, which blows northward in the warm sector. This intensifies and splits in two low-level jet (LLJ) branches during the day. The first one, flowing from the Tyrrhenian sea towards the Ligurian coast, is channelling warm moist (high θ_e values around or above 320 K) maritime air masses in a narrow band ahead of the cold front. This air mass is also relatively unstable with values of CAPE in the order of 500 Jkg^{-1} and has relatively low-convective inhibition. In this airstream, convection is triggered over the sea, by forced uplift over the Ligurian Apennines and later by the approach of the cold front. A second low-level jet blowing from south-east forms on the Po valley due to the blocking action of the orography on more stable air masses, a typical example of barrier wind (Buzzi et al. 2020). The mass convergence of these two branches in the western Po valley triggered high vertical velocities on the upwind side of the orography, generating intense and persistent orographic precipitation. A comparison with the radio sounding data from Ajaccio (Corsica) and San Pietro Capofiume (Emilia-Romagna region, Po valley), Milano Linate (Lombardy region, Po valley) confirms the different characteristics of the two airstreams with the Po valley LLJ being very shallow and stable although very intense, in the order of 20 m s^{-1} (not shown).

The 1994 Piedmont event was also characterized by a strong IVT band at the eastern flank of the upper-level trough (Fig. 3) with a magnitude constantly higher than the atmospheric river (AR) definition threshold of 250 kg s^{-1} m^{-1}. In addition, the total column water content

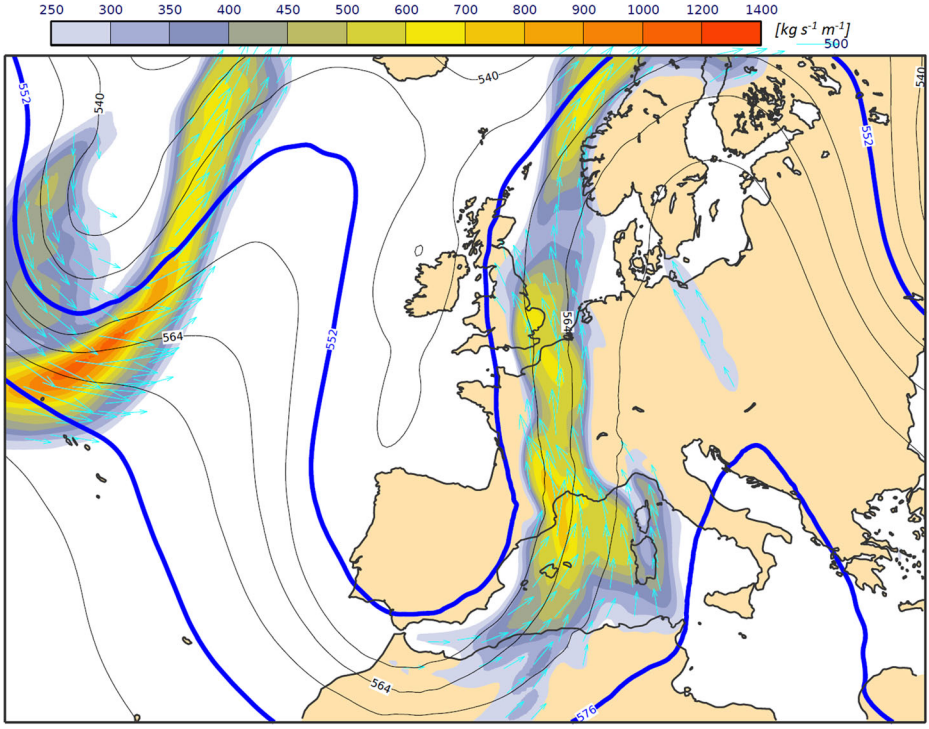

Fig. 3 Synoptic view of the 1994 Piedmont flood on 5 November 1994 00 UTC by the ERA5 reanalysis. Contours show geopotential height at 500 hPa (every 6 dam), the colour shading refers to the IVT magnitude [kg s^{-1} m^{-1}], and the cyan arrows indicate IVT vectors, drawn where the IVT magnitude exceeds the AR threshold of 250 kg s^{-1} m^{-1}

(TCWV) was greater than 20 kg m^{-2}. This allows us to affirm that the strong southerly moist flow ahead of the cold front can be classified as an AR, a circumstance also confirmed by Krichak et al. 2015.

As we have seen through the examination of the reanalysis fields, this event presents the key features that are typical of category 2 events, i.e., the abnormally strong flow from the south and the presence of both large-scale and deep convection precipitation peaks. The dynamic and thermodynamic characteristics of this event described herein agree with previous studies obtained with limited area model simulations (Ferretti et al. 2000, Cassardo et al. 2002). In particular, Cassardo et al. (2002) reported that the persistence of deep convection further contributed to the severity of the event over the Ligurian range.

4 Synoptic evolution and large-scale precursors

As stated above, the presence of a strong southerly airstream, classifiable as AR, is a crucial feature which characterizes this event as well as many other EPEs in the Alpine region. In this section, we discuss the origin and dynamical evolution responsible for its occurrence. For this purpose, we present two figures. Figure 4 shows the synoptic wave and the associated IVT on 4 November at 12 UTC, at the initial phase of the event. Figure 5 displays, in a compact way, the dynamical evolution of the upper-tropospheric flow and the associated Rossby wave packets (RWPs) which set the stage for the smaller-scale processes that eventually lead to the event. Figure 5 depicts the meridional wind component at 300 hPa, the corresponding envelope E, as well as the 2 PVU contour at 330 K on selected days leading to the event. The envelope field, diagnosed following Fragkoulidis et al. (2018), highlights the regions where the RWP amplitude is strong, i.e. the upper-tropospheric jet exhibits pronounced undulations.

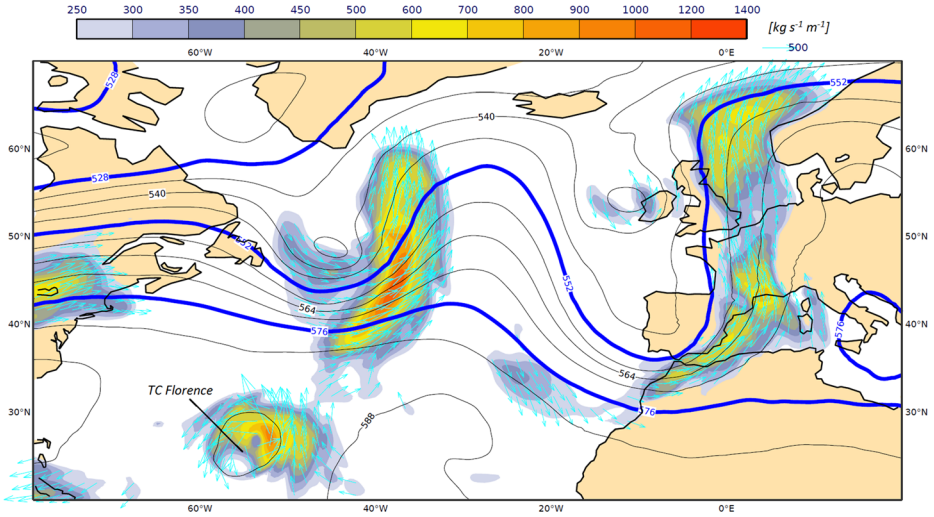

Fig. 4 Synoptic configuration on 4 November 1994 12UTC over the Atlantic basin. Contours show geopotential height at 500 hPa, every 6 dam, the colour shading refers to the IVT magnitude [kg s^{-1} m^{-1}] (see colour bar above), and the cyan arrows are IVT vectors, drawn only when the IVT magnitude exceeds the AR threshold of 250 [kg s^{-1} m^{-1}]

This is also reflected in the large meridional wind anomaly (v') values and the associated succession of troughs and ridges that result in a wavy 2 PVU contour.

The moist airstream that was crucial for the extreme precipitation event grew ahead and in response to a developing trough over the eastern Atlantic on 2 November (Fig. 5b). The narrow band of strong IVT associated with the trough can be identified in Fig. 3, where values exceeding the AR thresholds become evident already from 4 November (Fig. 4). Overall, the

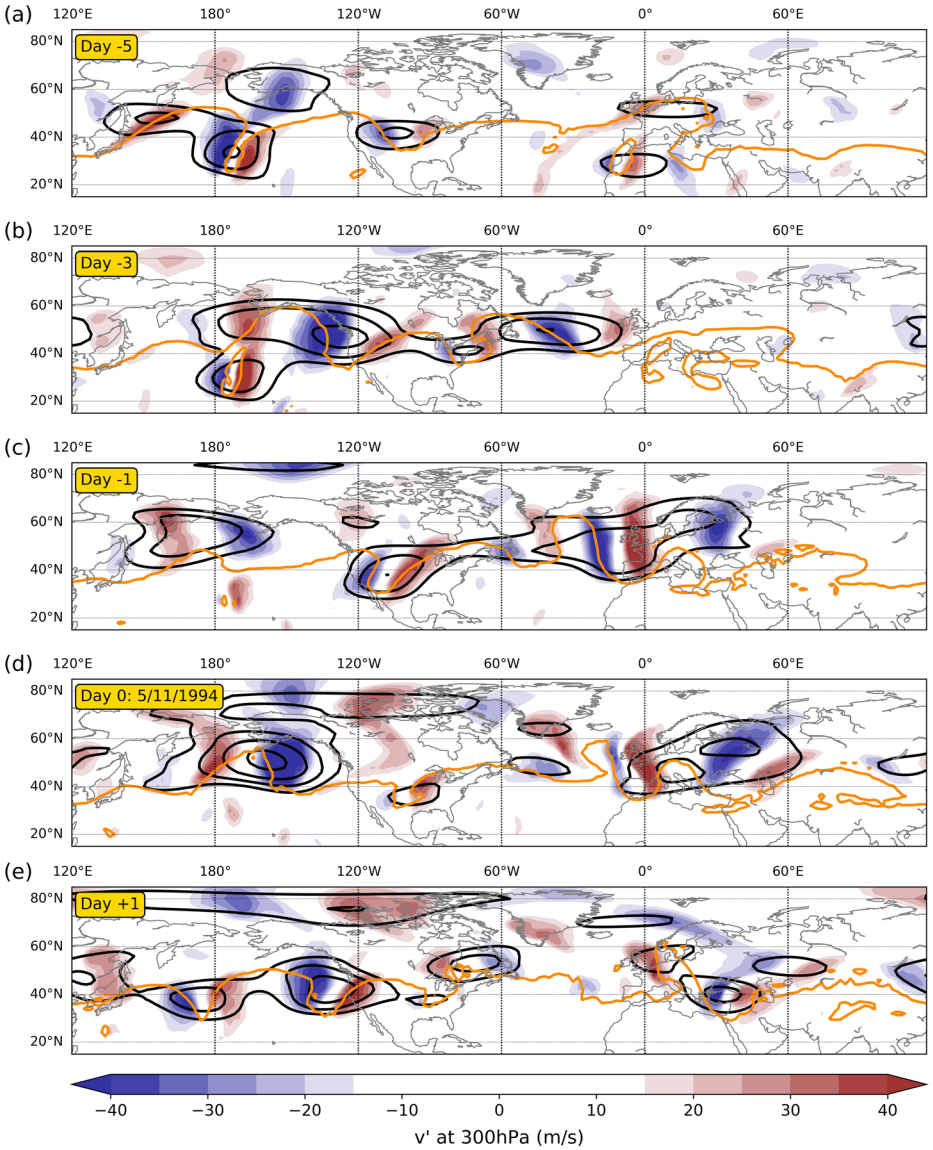

Fig. 5 Evolution of the upper-tropospheric flow leading to the November 1994 Piedmont flood. The panels depict mean daily values of meridional wind at 300 hPa (colour fill), the corresponding E at 300 hPa (black contours every 10 m/s starting from 25 m/s) and the 2 PVU isoline at 330 K (orange contour) at **a** 31 October 1994 (D-5), **b** 02 November 1994 (D-3), **c** 04 November 1994 (D-1), **d** 05 November 1994 (D0), and **e** 06 November 1994 (D+1). All maps show instantaneous values at 12 UTC

AR stretches from the Azores to the North Sea. In Fig. 4, the presence of hurricane Florence in the central Atlantic is also evident. A closer inspection of a sequence of snapshots around 4 November reveals that the circulation and moisture fluxes induced by Florence have interacted with the trough to the north and the associated upper-level jet. This may have indirectly influenced the evolution of the N. Atlantic wave packet propagating towards the Mediterranean. As can be seen from Fig. 4, there seems to be a connection in the IVT fluxes from the tropical cyclone to the trough in the central Atlantic, later visible in the wind field at 250 hPa (not shown). In this respect, as documented in several other occasions (Grams and Archambault 2016, Pohorsky et al. 2019), the low-PV air injection into the mid-latitude jet can cause a jet acceleration and a ridge building, thus strengthening the development of the trough downstream (in our case over the Mediterranean). A strong downstream development, possibly connected with anomalous water vapour fluxes in the upstream trough, is frequently observed in Cat2 events and this evolution is extensively investigated in Grazzini et al. (2020b).

In the following hours, the slow eastward movement and amplification of the synoptic wave pattern over Western Europe modulated a strong moisture transport and convergence towards the western Alpine region. This situation further intensified on 5 November, when the trough axis advanced slightly eastward, while the downstream ridge centred over the Adriatic Sea almost kept its position and amplified (Figs. 3, 5). Also note that at that time, a channelling of the AR between the largest Mediterranean islands (Sardinia and Corsica) and the continent is evident. This channelling may be responsible for the prefrontal precipitation during the night between 4 and 5 November. In Fig. 5 we note the northward expansion of the ridge in the orange PV contour on the Mediterranean, from 4 (panel c) to 5 November (panel d), presumably also affected by the low-PV outflow associated with the deep convection over northern Italy.

The synergic interaction between convection and the large-scale environment described above is typical of Cat2 events as discussed in G2020. It may arise from temporary positive feedback from the synoptic flow that, through mass convergence, favours local convection to grow into mesoscale systems, which in turn enhance low-PV air export into the upper levels, contributing to ridge amplification and further strengthening of mass convergence. However, the interaction of the large-scale flow and local mesoscale deep convective systems is not yet fully understood and deserves further investigation.

Finally, we briefly discuss the dynamical evolution of the RWP associated with the trough over the Mediterranean. The time reference (day 0, D0) is set on the day of maximum intensity, i.e. on 5 November at 12 UTC. On D-5, a RWP of large amplitude is located over the central Pacific, highlighted by the black contours (E) in Fig. 5a centred on a narrow PV streamer east of the dateline. On D-3 (2 November, panel b), the disturbance is growing and propagating rapidly over North America, inducing a new couplet (ridge-trough) development over the western North Atlantic, with the latter subsequently approaching western Europe. On D-1, the amplified trough remains over Western Europe and constitutes the stronger part of the RWP and the dominant flow feature associated with the EPE synoptic pattern. An apparent overturning and wave breaking between D0 and D+1 over eastern North Atlantic are well depicted by the 2 PVU contour. At the same time, v' and E get fragmented and imply an incoherent RWP at its decay stage.

This short analysis points to the remote origin of the RWP associated with the trough, which could be traced back to western-central Pacific 6 to 5 days before. The long lifetime and coherence of the wave packet may have played a role in determining the good predictability of

the large-scale flow in the medium-range forecasts, experienced even in the not so advanced operational systems of that time (Ferrero and Balsamo 2020). The statistical relation between long spatial and temporal coherence of RWPs and increased forecast skill was already reported by Grazzini and Vitart (2015).

5 Comparison with other similar EPEs

In this section, we compare this event to others that have recently affected the southern part of the Alpine area to identify analogies and threshold values for key features of the large-scale flow. As mentioned in several works (Ralph and Dettinger, 2011, Lavers and Villarini 2013, Krichak et al. 2015, Froidevaux and Martius, 2016), IVT represents an optimal integral variable to account for the large-scale contribution to the severity of a precipitation event. EPEs require extreme water vapour convergence to sustain high intensities for an extended period of time, which is why the association between precipitation and water vapour transport is particularly strong (Lavers et al. 2014). A first comparison of IVTe and IVTn in Table 2 shows that although moisture transport was significant in the 1994 event, it was inferior to the one registered during the Po flood of 11–15 October 2000. Precipitation in the 2000 event was, in fact, more intense, also due to the presence of higher convective instability (higher CAPE, lower DTmin, and higher column-integrated water vapour) associated with a warm air mass (see θ_e at 850 hPa in Table 2).

Aiming at comparing the contribution of the large-scale circulation, we display the distribution of IVTn as a tracer of the intensity of the upper-level wave and the availability of moisture. The distribution of IVTn, averaged over the target domain of northern-central Italy defined in G2020, is shown in Fig. 6 for the different EPE categories. Non-EPE days are shown in black, while Cat1, Cat2, and Cat3 events are coloured according to the legend. In addition, recent significant events are marked by the red bars on the *x*-axis. We notice that the

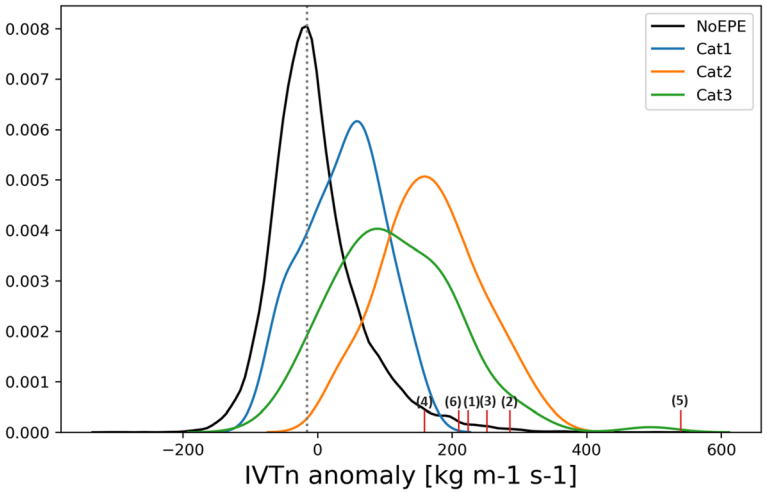

Fig. 6 Distribution of daily IVTn [kg m^{-1} s^{-1}] averaged over the target domain of Northern-Central Italy for non EPEs days (black curve), Cat1 days (blue curve), Cat2 days (orange curve), and Cat3 days (green curve). Numbers refer to analogue cases of the 1994 Piedmont event in chronological order. Recent cases are also considered not included in the former classification. (1) 5 November 1994, (2) 13 October 2000, (3) 14 October 2014, (4) 21 November 2016, (5) 20 October 2018 storm "Vaia", and (6) 21 October 2019

IVTn values associated with all the marked events lie around and mostly to the right of the Cat2 distribution mode, which is just slightly below 200 kg m^{-1} s^{-1}. All these events produced extensive and damaging floods over the western Po valley and the Piedmont region (see Arpa Piemonte 2019, for an intercomparison and description of these cases). Standing out from the Cat2 IVTn distribution is storm Vaia, one of the strongest ever recorded over Central and Northern Italy (Cavaleri et al. 2019). The Cat2 distribution is clearly separated from the non-EPE days distribution (black curve), so we can empirically assume that IVTn daily mean values beyond 200 kg m^{-1} s^{-1} are very likely for Cat2 events.

6 Discussion and conclusions

In this study, we have revisited the dynamical evolution of the 1994 Piedmont flood event with new reanalysis and high-resolution precipitation datasets and in the light of a recent EPE classification approach. We have shown that this event may be considered an archetype for southern Alpine Cat2 EPEs which are able to produce very high river discharges and widespread flooding on small and large river basins due to the combined presence of stratiform precipitation and deep convection. The main triggering factor was a meridionally elongated upper-level trough, embedded in an incoming Rossby wave packet that originated in the Pacific. The wave packet propagation modulated the transport of a large moisture quantity from the central Atlantic towards the Mediterranean, with a formation of an AR over the central Mediterranean Sea. We also documented the presence of hurricane Florence in the central Atlantic in the days before the events, which interacted with the upstream trough and arguably contributed to strengthen the downstream development of the synoptic wave responsible for the precipitation. Finally, we have highlighted the value of the integrated water vapour transport as a key variable for detecting large-scale conditions favourable to the realization of these events, proposing a threshold based on the meridional component IVTn.

There is a growing interest by forecasters to complement direct model precipitation output (including probability) with other variables/methods which could give a physical insight into the type of precipitation event to be expected. Lavers et al. (2016) pointed out that IVT is very useful to detect extreme events in the medium range or even later, while for the shorter forecast ranges, considering only water vapour fluxes may lead to higher false alarm rate than using precipitation. Therefore, we conclude that the increased predictability of water vapour transport could be used as the basis for a classification method, including other variables, e.g. related to RWP properties, to be applied to real-time forecast fields. This could provide a more robust approach to increase preparedness regarding EPEs, especially at longer forecast ranges. This is becoming even more substantial in view of the increasing likelihood of extreme precipitation events in a warming climate.

Acknowledgements We are grateful to three anonymous reviewers for their suggestions towards improving this study. We would also like to thank George Craig for useful discussions and suggestions on the manuscript.

Funding Open Access funding provided by Projekt DEAL.

Compliance with ethical standards

Competing interests The authors declare that they have no conflict of interest.

References

Arpa Piemonte 1998, L'evento alluvionale del 2–6 Novembre 1994. In Italian. Last accessed on 10/04/2020. http://www.arpa.piemonte.it/approfondimenti/temi-ambientali/geologia-e-dissesto/pubblicazioni/immagini-e-files/ev9496/EventialluvionaliinPiemonte1994cap1.pdf

Arpa Piemonte 2019, Eventi alluvionali in Piemonte - Evento del 19–24 ottobre 2019, prima parte. In Italian. Last accessed on 10/04/2020. http://www.arpa.piemonte.it/pubblicazioni-2/relazioni-tecniche/analisi-eventi/eventi2019/rapporto-evento-19-24-ottobre_partei

Buzzi A, Tartaglione N (1995) Meteorological modelling aspects of the Piedmont 1994 flood. MAP Newsletter 3:27–28

Buzzi A, Tartaglione N, Malguzzi P (1998) Numerical simulation of the 1994 Piedmont flood: role of orography and moist processes. Mon Weather Rev 126:2369–2383

Buzzi A, Di Muzio E, Malguzzi P (2020) Barrier winds in the Italian region and effects of moist processes. Bull of Atmos Sci& Technol 1:59–90. https://doi.org/10.1007/s42865-020-00005-6

Cassardo C, Loglisci N, Gandini D, Qian M, Niu G, Ramieri P, Pelosini R, Longhetto A (2002) The flood of November 1994 in Piedmont, Italy: a quantitative analysis and simulation. Hydrol Process 16(6):1275–1299. https://doi.org/10.1002/hyp.1062

Cavaleri L, Bajo M, Barbariol F, Bastianini M, Benetazzo A, Bertotti L, Chiggiato J, Davolio S, Ferrarin C, Magnusson L, Papa A, Pezzutto P, Pomaro A, Umgiesser G (2019) The October 29, 2018 storm in Northern Italy – an exceptional event and its modeling, Progress in oceanography. 178:102178. https://doi.org/10.1016/j.pocean.2019.102178

Ferrero E., G. Balsamo (2020), The 1994 Piedmont flood revisited. ECMWF Newsletter 162, Winter 2020, pag. 8–9

Ferretti R, Low-Nam S, Rotunno R (2000) Numerical simulations of the 1994 Piedmont flood of 4-6 November. Tellus 52A:162–180

Fragkoulidis G, Wirth V, Bossmann P, Fink AH (2018) Linking northern hemisphere temperature extremes to Rossby wave packets. Q J R Meteorol Soc 144(711):553–566. https://doi.org/10.1002/qj.3228

Froidevaux P, Martius O (2016) Exceptional integrated vapour transport toward orography: an important precursor to severe floods in Switzerland. Q.J.R. Meteorol. Soc. 142:1997–2012. https://doi.org/10.1002/qj.2793

Grams C, Archambault H (2016) The key role of diabatic outflow in amplifying the midlatitude flow: a representative case study of weather systems surrounding western North Pacific extratropical transition. Mon Weather Rev 144(10):3847–3869. https://doi.org/10.1175/MWR-D-15-0419.1

Grazzini F (2007) Predictability of a large-scale flow conducive to extreme precipitation over the western Alps. Meteorog Atmos Phys 95(3–4):123–138. https://doi.org/10.1007/s00703-006-0205-8

Grazzini F, Vitart F (2015) Atmospheric predictability and Rossby wave packets. Q.J.R. Meteorol Soc 141: 2793–2802. https://doi.org/10.1002/qj.2564

Grazzini F, Craig G, Keil C, Antolini G, Pavan V (2020a) Extreme precipitation events over Northern Italy. Part I: A systematic classification with machine-learning techniques Quarterly Journal of the Royal Meteorological Society 146:69–85. https://doi.org/10.1002/qj.3635

Grazzini, F. , Fragkoulidis, G., Teubler, F., Wirth, V., Craig G. C. (2020b): Extreme precipitation events over Northern-Central Italy. Part II: Dynamical precursors and decadal variability. *Submitted to QJRMS*

Hersbach, H., B. Bell, P. Berrisford, S. Hirahara, A. Horanyi, J. Muñoz-Sabater, J. Nicolas, C. Peubey, R. Radu, D. Schepers, A. Simmons, C. Soci, S. Abdalla, X. Abellan, G. Balsamo, P. Bechtold, G. Biavati, J. Bidlot, M. Bonavita, G. Chiara, P. Dahlgren, D. Dee, M. Diamantakis, R. Dragani, J. Flemming, R. Forbes, M. Fuentes, A. Geer, L. Haimberger, S. Healy, R. J. Hogan, E. Holm, M. Janiskova, S. Keeley, P. Laloyaux, P. Lopez, C. Lupu, G. Radnoti, P. Rosnay, I. Rozum, F. Vamborg, S. Villaume, and J. Thepaut, 2020: The ERA5 global reanalysis. Quarterly Journal of the Royal Meteorological Society, qj.3803, URL https://doi.org/10.1002/qj.3803

Krichak SO, Barkan J, Breitgand JS, Gualdi S, Feldstein SB (2015) The role of the export of tropical moisture into midlatitudes for extreme precipitation events in the Mediterranean region. Theor Appl Climatol 121: 499–515. https://doi.org/10.1007/s00704-014-1244-6

Lavers DA, Villarini G (2013) The nexus between atmospheric rivers and extreme precipitation across Europe. Geophys Res Lett 40:3259–3264. https://doi.org/10.1002/grl.50636

Lavers DA, Pappenberger F, Zsoter E (2014) Extending medium-range predictability of extreme hydrological events in Europe. Nat Commun 5:5382

Lavers DA, Waliser DE, Ralph FM, Dettinger MD (2016) Predictability of horizontal water vapor transport relative to precipitation: enhancing situational awareness for forecasting western U.S. extreme precipitation and flooding. Geophys Res Lett 43:2275–2282. https://doi.org/10.1002/2016GL067765

Martius O, Schwierz C, Davies HC (2008) Far-upstream precursors of heavy precipitation events on the Alpine south-side. Q J R Meteorol Soc 134(631):417–428. https://doi.org/10.1002/qj.229

Owens, R G, Hewson, T D (2018): ECMWF Forecast User Guide. Reading: ECMWF. https://doi.org/10.21957/m1cs7h

Pavan V, Antolini G, Barbiero R, Berni N, Brunier F, Cacciamani C, Cagnati A, Cazzuli O, Cicogna A, de Luigi C, di Carlo E, Francioni M, Maraldo L, Marigo G, Micheletti S, Onorato L, Panettieri E, Pellegrini U, Pelosini R, Piccinini D, Ratto S, Ronchi C, Rusca L, Sofia S, Stelluti M, Tomozeiu R, Torrigiani Malaspina T (2019) High resolution climate precipitation analysis for North-Central Italy, 1961–2015. Clim Dyn 52(5–6):3435–3453. https://doi.org/10.1007/s00382-018-4337-6

Pohorsky R, Röthlisberger M, Grams C, Riboldi J, Martius O (2019) The climatological impact of recurving north Atlantic tropical cyclones on downstream extreme precipitation events. Mon Weather Rev 147(5): 1513–1532. https://doi.org/10.1175/MWR-D-18-0195.1

Ralph FM, Dettinger MD (2011) Storms, floods, and the science of atmospheric rivers, EOS, transactions. Am Geophys Union 92(32):265–272